



Groundwater Aquifer Vulnerability Assessment using a Dar-Zarrouk Parameter in a Proposed Aboru Residential Estate, Lagos State, Nigeria

AYUK, MA

Department of Applied Geophysics, Federal University of Technology, Akure, Nigeria.
*Email: ayukmike2003@yahoo.com; Tel.: +2348035223352

ABSTRACT: The need to build an automobile mechanic settlement, abattoir and a proposed meat processing factory at Aboru residential estate necessitated a geophysical assessment (using a Dar-Zarrouk parameter – longitudinal unit conductance, S) of the vulnerability of the subsurface aquifers in the study area against the expected long-term anthropogenic impacts of these facilities on the groundwater system. Thirteen (13) Vertical Electrical Sounding (VES) points and four (4) Dipole-Dipole resistivity profile lines were occupied on four traverse lines across the study area. Isoresistivity and Isopach maps were generated and Total Longitudinal Unit Conductance, S of the earth materials overlying the aquifer was computed and the aquifer protective capacity (APC) map was generated. The VES delineated four (4) geo-electric layers namely; topsoil, pebbly/lateritic sand, clay/clayey/silty sand and sandstone. The depth to the sandstone aquifer ranges from 30.6 – 39.4 m with resistivity values ranging from 851 – 1437 Ωm . The iso-resistivity and isopach maps reveal that the near surface lateritic materials with resistivity values ranging from 350 – 1150 Ωm and thicknesses ranging from 2 – 29 m are pervious. The Total Longitudinal Unit Conductance, S varies from 0.0164 - 0.1168 mhos indicating a poor to weak protective capacity rating across the study area and the APC map reveals that the north-eastern and western parts of the study area show areas with weak protective capacity ratings while other areas are characterized by poor protective capacity rating. As such, the establishment of the proposed service facilities in the study area is strongly discouraged as the nature of their operations has a high potential to contaminate and eventually pollute the sub-surface aquifers on the long-run. If however the inevitability of their establishment cannot be set-aside, then secondary measures must be taken to forestall a direct impact of their operations on the subsurface.

DOI: <https://dx.doi.org/10.4314/jasem.v23i12.2>

Copyright: Copyright © 2019 Ayuk. This is an open access article distributed under the Creative Commons Attribution License (CCL), which permits unrestricted use, distribution, and reproduction in any medium, provided the original work is properly cited.

Dates: Received: 04 October 2019; Revised: 11 November 2019; 23 November 2019

Keywords: Aquifer, Dar-Zarrouk, Vulnerability, Longitudinal Unit Conductance

The geoelectrical resistivity method has been successfully employed in the delineation of subsurface geological sequence, geological structures/features of interest, aquifer units, types and depth extent in almost all geological terrains (Oladapo *et al.* 2004; Ako *et al.* 2005; Lashkaripour *et al.*, 2005; Hassanein *et al.* 2007). This is because of the significant resistivity contrasts that exist between different earth materials (Olorunfemi and Fasuyi 1993). The resistivity method can therefore map interface along which a resistivity contrast exists. This interface may or may not coincide with geological boundary (Telford *et al.* 1990). In addition, vertical electrical sounding (VES) has been widely used to evaluate groundwater potentials and area of high groundwater yield (Ako and Osondu 1986; Abdulaziz 2005; Abiola *et al.* 2009). Geoelectrical methods are also used extensively in groundwater mapping for investigation of the vulnerability of shallow aquifers (Abiola *et al.* 2009). The vulnerability of aquifers is largely dependent on the presence or absence of protective impermeable layer, usually clay. The earth medium acts as a natural filter to percolating fluid; its ability to retard and filter percolating fluid is a measure of its protective capacity

(Olorunfemi *et al.*, 1998). Studies such as Sørensen *et al.* (2005) have shown that geoelectrical method is an invaluable tool in mapping aquifer vulnerability because of its capability to distinguish low- and high-resistive formations. The concept of groundwater vulnerability is based on the assumption that the physical environment may provide some degree of protection to groundwater against natural impacts, especially with regard to contaminants entering the subsurface zone. Consequently, some land areas are more vulnerable to groundwater contamination than others. Henriet (1976) showed that the combination of layer resistivity and thickness in the Dar Zarrouk parameters S (longitudinal conductance) and T (transverse resistance) may be of direct use in aquifer protection studies and for the evaluation of hydrologic properties of aquifer. The protective capacity is considered to be proportional to the longitudinal unit conductance in mhos (Olorunfemi *et al.*, 1998; Oladapo *et al.*, 2004; Ayolabi, 2005 and Atakpo and Ayolabi, 2009).

Aboru mini-estate is a large densely populated residential area of Lagos whose sources of water are

*Email: ayukmike2003@yahoo.com; Tel.: +2348035223352

three industrial groundwater boreholes that tap the groundwater from a deep seated sandstone/sand aquifer at three strategic locations in the estate. Automobile mechanic settlement, abattoir and meat processing factory have been proposed to be established in the estate due to urbanization and self-sustainability of the area. The operations of these service facilities have high potential to contaminate and pollute the sub-surface aquifers in the study area on the long-run due to the possibility of indiscriminate dumping of waste on the ground surface from these facilities. This therefore has necessitated the aquifer vulnerability study in the study area. In this study therefore, 2D dipole-dipole and 1D vertical electrical sounding (VES) geophysical techniques were applied to determine the first order geoelectric parameters (resistivity ρ and thickness h) to delineate the depth to aquifer and its lateral extent and a second order geoelectric parameter (longitudinal unit conductance) to determine the aquifer protective capacity.

MATERIALS AND METHODS

Study area: Geologically, Lagos state falls within Eastern Dahomey Basin. The stratigraphy of Cretaceous to Tertiary sedimentary sequence of the Eastern Dahomey Basin is divided into: Abeokuta Group, Imo Group, Ilaro Formation, Benin Formation, Coastal plain sands and recent alluvium (Omatsola and Adegoke, 1981). The study area is underlain by the Coastal Plain Sands of Lagos (Fig. 1). Aboru (Fig. 2) is located in Iyana-Ipaja area of Lagos, southwestern Nigeria. It lies between Northing 732983mN and 733097mN and Easting 530651mE and 530771mE (Fig. 2). The two prevailing climatic seasons are the dry (November to March) and wet (April to October) seasons and it is found in the rain forest environment with mean annual rainfall ranging between 1500 mm and 2500 mm (Balogun, 2000).

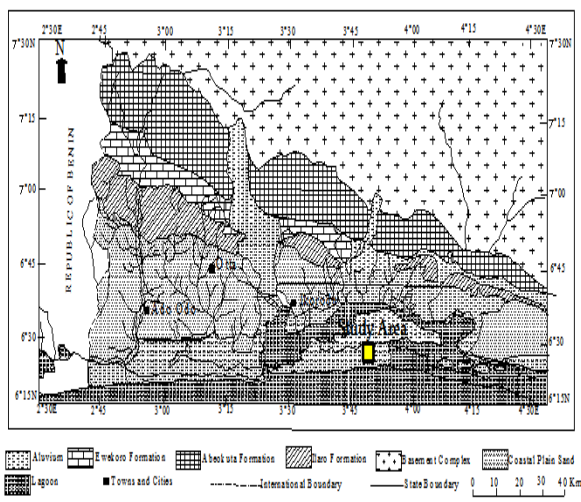


Fig 1: Regional map of the study area (Kogbe, 1976)

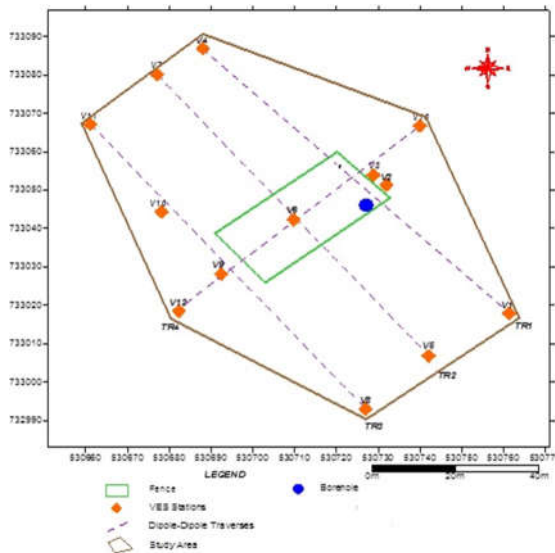


Fig 2: Base map of the study area

Data Acquisition: Geophysical Investigation: 2D dipole-dipole electrical resistivity measurements were taken along four (4) traverses using the R-50 Soil Test Resistivity Meter. Traverses 1-3 run in SE-NW direction while traverse 4 runs in approximately SW-NE direction (Fig. 2). Electrode separation of 5 m and inter-dipole expansion factor (n) was varied from 1-5 along the four traverses. Traverse 1-3 each have a total surface length of 100 m while traverse 4 has a total surface length of 80 m. Following the 2D dipole-dipole measurement, a total of thirteen (13) VES data were acquired within the study area using the Schlumberger Array type. Four VES points (V1 to V4) were on TR1, three VES points (V5 to V7) on TR2, four VES points (V8 to V11) on TR3 and two VES points (V12 to V13) on TR4 as shown in figure 2. The highest half-current electrode spread length ($AB/2$) is 65 m.

Data Processing: Geophysical Investigation: The 2D Dipole-Dipole data sets were processed for inversion with DiproWin Software to generate the pseudo sections and calculate the true resistivity distribution within the area. Anomalous resistivity points were identified across the sections and these were later occupied with the VES. The VES sounding curves so generated were processed with partial curve matching to quantitatively generate the first order geoelectric parameters. These were used as input parameters for inversion using WINRESIST iteration software. Spatial correlations of the resistivity, thickness and depth were used to generate the geoelectric sections along the traverses.

Dar-Zarrouk Parameters: Dar-Zarrouk (D-Z) parameters were defined by Maillat (1947). T is the

resistance normal to the face and S is the conductance parallel to the face for a unit cross section area, which plays an important role in resistivity soundings. D-Z parameters are sufficient for computing the distribution of surface potential and hence an electrical resistivity graph (Henriet 1976).

Suppose that a section consists of N fine layers with thickness h_1, h_2, \dots, h_n and resistivity $\rho_1, \rho_2, \rho_3, \dots, \rho_n$ for a block of unit square area and thickness $H = \sum_{i=1}^N h_i$

These values of S and T are set equal to those for an anisotropic block with unit square area. So that: Longitudinal Unit Conductance S,

$$S = \frac{h_1}{\rho_1} + \frac{h_2}{\rho_2} + \frac{h_3}{\rho_3} + \dots + \frac{h_n}{\rho_n} = \sum_{i=1}^N \frac{h_i}{\rho_i} \dots 1$$

Transverse Unit Resistance T,

$$T = \rho_1 h_1 + \rho_2 h_2 + \rho_3 h_3 + \dots + \rho_n h_n = \sum_{i=1}^N \rho_i h_i \dots 2$$

Longitudinal Resistivity R_s ,

$$R_s = \frac{H}{S} \dots \dots \dots 3$$

Transverse Resistivity, R_T

$$R_T = \frac{T}{H} \dots \dots \dots 4$$

In this study however, only the Longitudinal Unit Conductance S in mhos (Equation 2) was considered as it is found to be proportional to the protective capacity of the overburden (Olorunfemi *et al.*, 1998; Oladapo *et al.*, 2004. Ayolabi, 2005 and Atakpo and Ayolabi, 2009).

RESULTS AND DISCUSSION

Geophysical Investigation: **2D Resistivity Imaging:** Figs. 3-6 present the 2D resistivity structure for traverse 1 – 4. Traverse 1-3 are oriented in the SE-NW direction (Figs. 3-5). Traverse 4 is oriented in SW-NE direction (Fig. 6). In SE-NW direction (Figs. 3-5), lateral distance of 90 m was covered and a depth of 15 m was imaged. Resistivity varies from 70 to 1047 Ωm across traverses 1 – 3 in this orientation. Resistivity distribution across this direction reveals two distinct resistivity structures indicating clayey/clayey sand/sandy topsoil (with an indication of being lateritic on traverse 2) and lateritic sand (which is likely to be pebbly in nature). Topsoil resistivity and thickness range from 70 – 825 Ωm and 2 – 3 m respectively. The resistivity and thickness of the lateritic sand range from 477 (in traverse 2) – 1047 Ωm (in traverse 1) and 12 – 13 m.

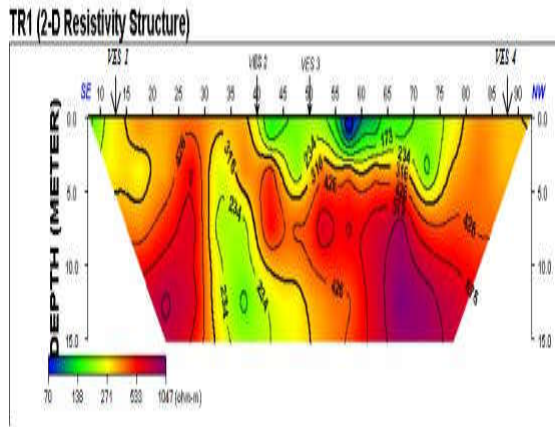


Fig 3: 2-D resistivity structure along traverse 1 in SE-NW direction

Across these traverses 1 – 3, resistivity signatures are fairly similar and subsurface parameters are fairly uniform because the traverses orient in the same direction i.e SE-NW (Fig. 2). Across these traverses (1-3) in this direction and at 15 m depth, there seems to be no resistivity structure that could be of good hydrogeological significance for groundwater exploitation.

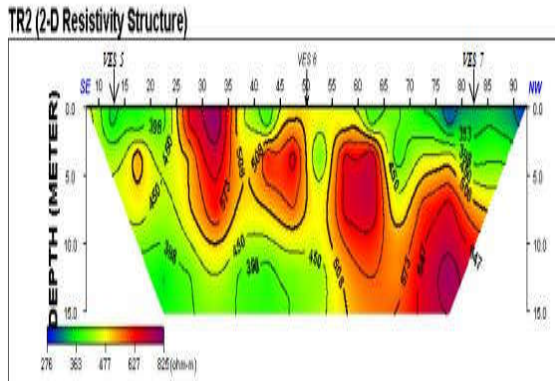


Fig 4: 2-D resistivity structure along traverse 2 in SE-NW direction

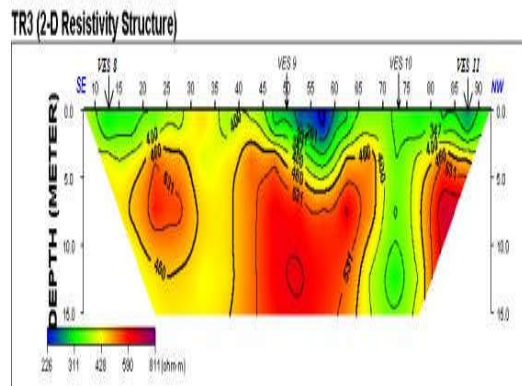


Fig 5: 2-D resistivity structure along traverse 3 in SE-NW direction

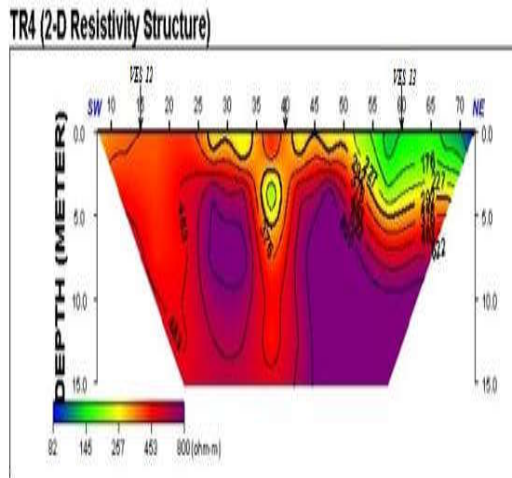


Fig 6: 2-D resistivity structure along traverse 4 in SW-NE direction

In SW-NE direction is traverse 4 (Figs. 2 and 6). Lateral distance of 70 m was covered and depth of 15 m was imaged (Fig. 6). The resistivity distribution along this traverse shows three distinct resistivity structures indicating the topsoil, clayey sand and lateritic sand. The topsoil, which is sandy in nature (with resistivity ranging from 227 – 483 Ωm) is fairly continuous across the traverse up to 50 m lateral distance (Fig. 6). Beyond here, the topsoil is clayey sand with resistivity ranging from 145 – 176 Ωm . The thickness of the topsoil ranges from 2 – 5 m. The topsoil is underlain by a lateritic sand layer with resistivity and thickness ranging from 622 - 800 Ωm and 5 – 10 m. The lateritic sand is not fairly continuous in the subsurface based on the resistivity distribution (Fig. 6). At the maximum depth of 15 m imaged, there is no indication of an aquifer.

1D Vertical Electrical Sounding (VES): The field curves obtained within the study area are the AK, KH, KQ, AKH, KHK and KHKH types with the AK-type being dominant. The AK curve type accounted for about 61.5% while the remaining curve types each accounted for 7.7% of the total curve types within the study area. Frequency distribution of the curve types is presented in Fig. 7 and a typical curve type from each traverse is presented in Fig. 8. The summary of the VES results is presented in Table 1. From the VES curves, four (4) to six (6) layers were delineated indicating topsoil, lateritic sand, pebbly sand, silty/clayey sand and sandstone. VES 11 reveals six (6) layers, VES 3 and 11 reveal five (5) layers while other VES curves reveal 4 layers. On traverse 1 (Fig. 9) are VES 1-4. Four (4) to five (5) layers are delineated along this traverse with four (4) layers in VES 1, 2 and 4 and five (5) layers in VES 3.

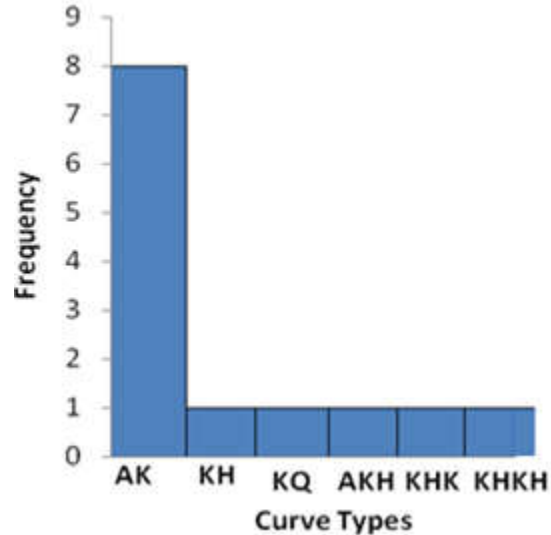


Fig. 7: Histogram of the curve types obtained in the study area

The topsoil, whose resistivity and thickness range from 25 – 135 Ωm and 0.7 – 1.1 m is underlain by pebbly sand in VES 1, 3 and 4 and by lateritic sand in VES 2 (Fig. 9). The resistivity and thickness of the pebbly sand range from 284 – 346 Ωm and 0.9 – 6.6 m in VES 1, 3 and 4 while in VES 2, the resistivity and thickness of the lateritic sand are 2526 Ωm and 0.9 m. The third layer in VES 1, 3 and 4 is the lateritic sand with resistivity and thickness ranging from 494 – 1172 Ωm and 3.9 – 23.4 m while in VES 2, the third layer is the pebbly sand with resistivity and thickness of 498 Ωm and 2.4. Layer four along this traverse is silty sand across VES 1, 2 and 3. At VES 4, the fourth layer is clayey sand. The resistivity of the silty sand varies from 173 – 298 Ωm and its thickness is 28.2 m in VES 3 only. The resistivity of the clayey sand is 100 Ωm . The thickness could not be determined because the current terminated at this zone. VES 3 is underlain by a fifth layer (Fig. 6) of sandstone with resistivity of 858 Ωm , whose thickness could not be determined because the current terminated at this zone and the sandstone is suspected to be an aquifer of good hydrogeological significance. On traverse 2 (Fig. 10) are VES 5 – 7. Four (4) layers are delineated along this traverse. The topsoil, with resistivity and thickness ranging from 131 – 242 Ωm and 0.8 – 1.8 m is underlain by lateritic sand in VES 5 and 6 with resistivity and thickness varying from 601 – 966 Ωm and 0.6 – 1.5 m while in VES 7, the topsoil is underlain by pebbly sand with resistivity 285 Ωm and thickness 5 m respectively. The third layer on this traverse is silty sand, pebbly sand and lateritic sand on VES 5, 6 and 7 with corresponding resistivity 374 Ωm & thickness 27.4 m, 573 Ωm & 12.2 m and 639 Ωm and 13.3 m respectively.

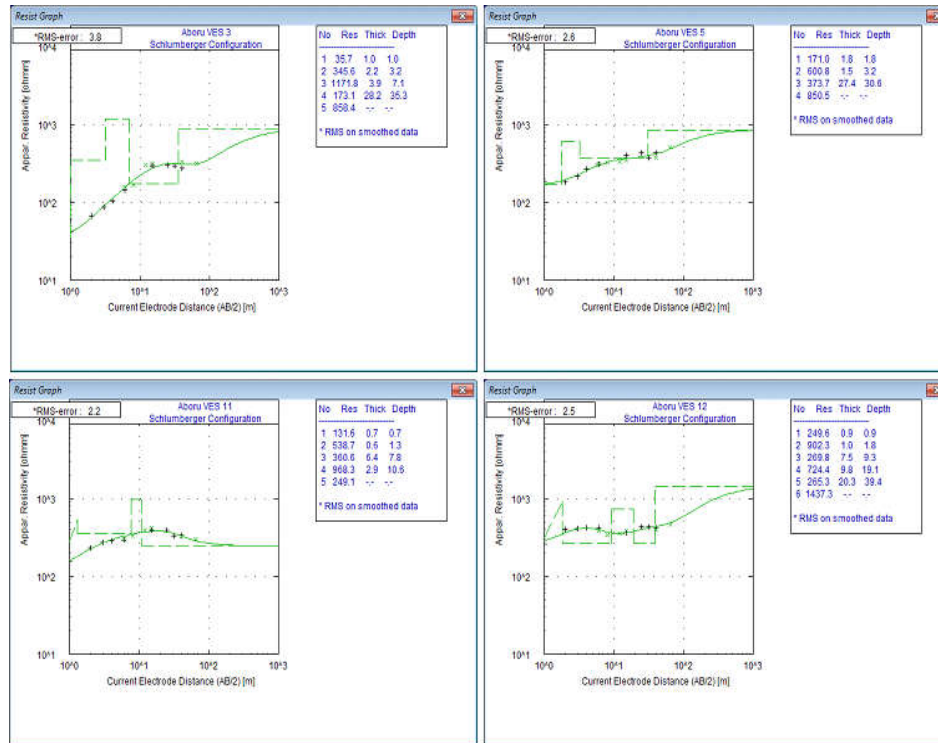


Fig. 8: Typical VES curve-type from each traverse 1-4

The third layer is underlain by sandstone in VES 5 and in VES 6 and 7; it is underlain by silty sand (Fig. 10). The resistivity of the sandstone is 851 Ω m while the resistivity of the silty sand varies from 264 – 372 Ω m in VES 6 and 7. Their thicknesses could not be determined because the current terminated at that depth. The sandstone at VES 5 is an aquifer. On traverse 3 (Fig. 11) are VES 8, 9, 10 and 11. Four (4) layers are delineated on this traverse.

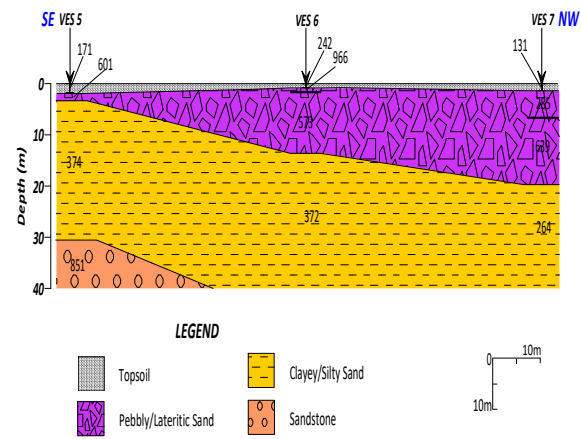


Fig. 10: Geoelectric section along traverse 2

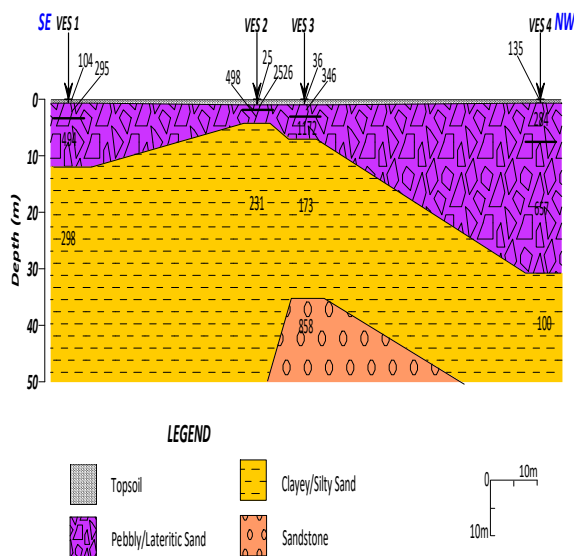


Fig. 9: Geoelectric section along traverse 1

The topsoil, with resistivity and thickness ranging from 132 – 297 Ω m and 0.7 – 1.7 m is underlain by pebbly sand in VES 8 and 9 with resistivity and thickness varying from 314 – 569 Ω m and 4.6 – 5.0 m while in VES 10 and 11, the topsoil is underlain by lateritic sand with resistivity and thickness varying from 539 - 610 Ω m and 0.6 -1.7 m respectively. The third layer on this traverse is lateritic sand, on VES 8 and 9 with corresponding resistivity and thickness varying from 638 - 1185 Ω m and 16.6 – 22.2 m, while in VES 10 and 11 the third layer is silty sand and pebbly sand with resistivity and thickness of 391 Ω m and 38.9 m for the silty sand and 361 Ω m and 6.4 m for the pebbly sand respectively.

Table 1: Summary of the VES Interpretation Results

VES No.	Curve Type	No. of Layers	Resistivity Value (Ωm)	Thickness (m)	Depth (m)	Inferred Lithology	Hydrogeological Significance
1	AK	1	104	0.8	0.8	Topsoil	
		2	295	2.7	3.5	Pebbly Sand	
		3	494	8.5	12.0	Lateritic Sand	
		4	298	-	-	Silty Sand	
2	AK	1	25	1.1	1.1	Topsoil	
		2	2526	0.9	1.9	Lateritic Sand	
		3	498	2.4	4.3	Pebbly Sand	
		4	231	-	-	Silty Sand	
3	AKH	1	36	1.0	1.0	Topsoil	
		2	346	2.2	3.2	Pebbly Sand	
		3	1172	3.9	7.1	Lateritic Sand	
		4	173	28.2	35.3	Silty Sand	
		5	858	-	-	Sandstone	Aquifer
4	AK	1	135	0.7	0.7	Topsoil	
		2	284	6.6	7.4	Pebbly Sand	
		3	657	23.4	30.8	Lateritic Sand	
		4	100	-	-	Clayey Sand	
5	KH	1	171	1.8	1.8	Topsoil	
		2	601	1.5	3.2	Lateritic Sand	
		3	374	27.4	30.6	Silty Sand	
		4	851	-	-	Sandstone	Aquifer
6	AK	1	242	0.8	0.8	Topsoil	
		2	966	0.6	1.4	Lateritic Sand	
		3	573	12.2	13.6	Pebbly Sand	
		4	372	-	-	Silty Sand	
7	AK	1	131	1.5	1.5	Topsoil	
		2	285	5.0	6.5	Pebbly Sand	
		3	639	13.3	19.8	Lateritic Sand	
		4	264	-	-	Silty Sand	
8	AK	1	297	1.5	1.5	Topsoil	
		2	314	5.0	6.6	Pebbly Sand	
		3	1185	16.6	23.2	Lateritic Sand	
		4	64	-	-	Clay	
9	AK	1	140	1.0	1.0	Topsoil	
		2	569	4.6	5.6	Pebbly Sand	
		3	638	22.2	27.6	Lateritic Sand	
		4	136	-	-	Clayey Sand	
10	KQ	1	156	1.7	1.7	Topsoil	
		2	610	3.0	4.7	Lateritic Sand	
		3	391	38.9	43.6	Silty Sand	
		4	330	-	-	Clayey Sand	
11	KHK	1	132	0.7	0.7	Topsoil	
		2	539	0.6	1.3	Lateritic Sand	
		3	361	6.4	7.8	Pebbly Sand	
		4	968	2.9	10.6	Lateritic Sand	
		5	249	-	-	Silty Sand	
12	KHKH	1	250	0.9	0.9	Topsoil	
		2	902	1.0	1.8	Lateritic Sand	
		3	270	7.5	9.3	Pebbly Sand	
		4	724	9.8	19.1	Lateritic Sand	
		5	265	20.3	39.4	Silty sand	
		6	1437	-	-	Sandstone	Aquifer
13	AK	1	15	0.6	0.6	Topsoil	
		2	176	5.9	6.6	Pebbly Sand	
		3	393	17.0	23.6	Lateritic Sand	
		4	81	-	-	Clayey Sand	

The fourth layer in VES 8 is clay with resistivity of 64 Ωm and in VES 9 and 10, the fourth layer is the clayey sand with resistivity ranging from 136 to 330 Ωm . The thickness of this fourth layer could not be determined at these three VES locations because the current terminated in this zone. At VES 11, the fourth layer is lateritic sand with resistivity and thickness of 968 Ωm

and 2.9 m. This layer is underlain by silty sand of resistivity 249 Ωm . The thickness could not be determined because the probing current terminated at this zone. On this traverse, there is no indication of the presence of an aquifer in the subsurface within the depth of investigation.

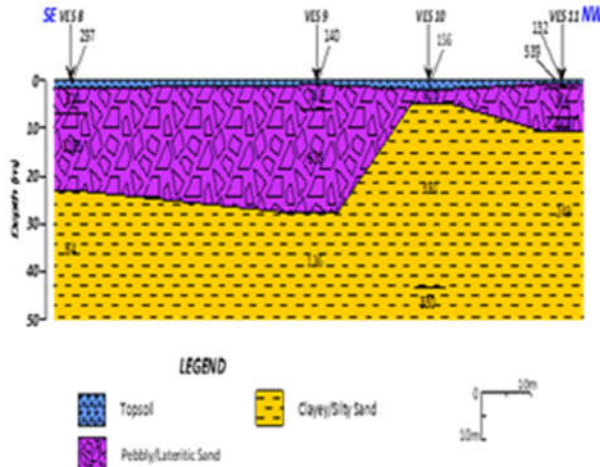


Fig. 11: Goelectric section along traverse 3

On traverse 4 (Fig. 12) are VES 12 and 13. On this traverse are VES 9, 6 and 3 (Fig. 2) in a co-occurrence due to traverse orientation (which has been discussed earlier and singly on their respective traverses). Four (4) and six (6) layers are delineated on VES 12 and 13 respectively. The topsoil, with resistivity and thickness ranging from 15 – 250 Ω m and 0.6 – 0.9 m is underlain by lateritic sand in VES 12 with resistivity and thickness 902 Ω m and 1.0 m while in VES 13, the topsoil is underlain by pebbly sand with resistivity and thickness of 176 Ω m and 5.9 m respectively. The third layer in VES 12 is pebbly sand with resistivity and thickness of 270 Ω m and 7.5 m. In VES 13, the third layer is lateritic sand with 393 Ω m and 17 m resistivity and thickness values respectively.

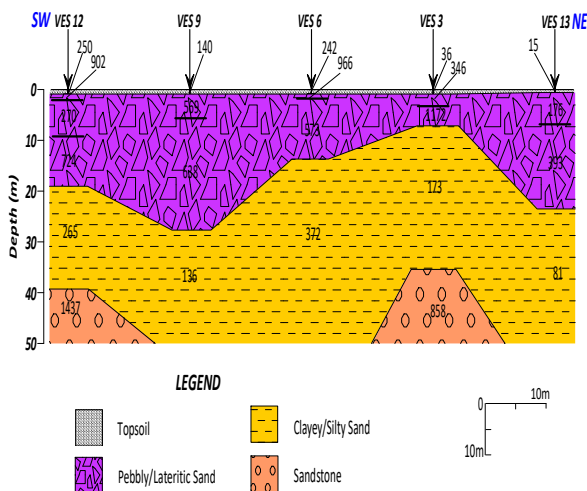


Fig. 12: Goelectric section along traverse 4

The fourth layer in VES 12 is lateritic sand with resistivity and thickness values of 724 Ω m and 9.8 m while the fourth layer in VES 13 is clayey sand with resistivity of 81 Ω m. The thickness could not be determined because the current terminated at this

point. The fifth layer in VES 12 is silty sand having resistivity and thickness values of 265 Ω m and 20.3 m respectively. The fifth layer is sandstone (Fig. 6d) with resistivity of 1437 Ω m but the thickness could not be determined because the probing current terminated at this point. The sandstone here is suspected to be of good hydrogeological significance. These results from the geoelectric sections correlate with the results from the 2D electrical resistivity sections (Fig. 3 – 6). The 1D geoelectric investigation only images deeper depths than the 2D electrical resistivity investigation. There is a strong indication that the basal sandstone layer delineated by 1D geoelectric investigation at depth is the most suitable aquifer in the study area capable of supporting groundwater exploitation. The nature of the near-surface geologic materials overlying the aquifer is relatively porous and permeable thus offering little or no protection over the aquifer against contamination of any kind.

Iso-resistivity and Iso-pach Mapping of the Subsurface: Isoresistivity map of the subsurface layer (pebbly/lateritic sand) underlying the topsoil is presented in figure 13. The layer’s average resistivity ranges from 350 to 1150 Ω m. An almost uniform resistivity of < 750 Ω m is observed in the study area (Fig. 13). A closure of high resistivity ranging from 750 - 1500 Ω m is revealed in the south eastern part of the study area (Fig. 13) and this is typical of the highly resistive (but permeable) pebbly/lateritic sand delineated as the second layer in the geoelectric sections (Fig. 9-12) overlying the sandstone aquifer at depth. Isopach map of the second layer, which is the pebbly/lateritic sand, is presented in figure 14. The map shows a variation in the thickness of the pebbly/lateritic sand second layer within the study area. The thickness varies from 1 - 31 m (Fig. 14). In the NE-SW direction and slightly at the centre of the study area, the thickness varies from 13 – 31 m. This result is indicated in the geoelectric section for traverse 4 (Fig. 12).

In NW – SE direction, the layer thickness varies from 1-11 m as also indicated in the geoelectric section for traverse 1-3 (Figs. 9 - 11). The relative thickness of the pebbly/lateritic sand; second layer in the study area does not give a protection to the underlying aquifer because of being a porous and permeable geologic material.

Evaluation of Aquifer Protective Capacity: Aquifer protective capacity (APC) is the ability of the overlying layers of rock (i.e the overburden) above the aquifer unit to impede, slow-down, filter and contain percolating ground surface contaminating fluids and run-offs.

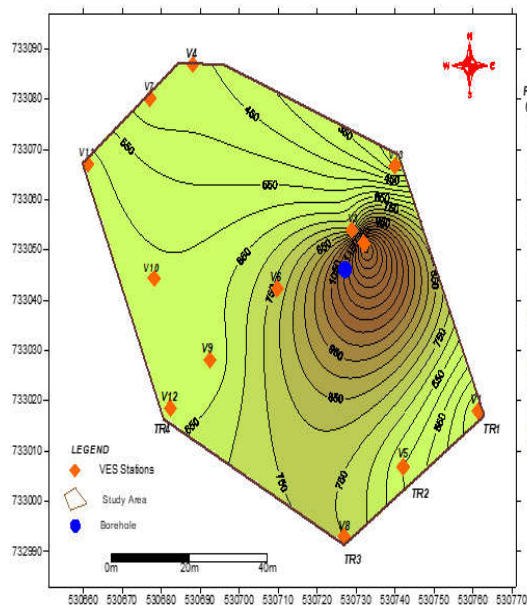


Fig. 13: Iso resistivity Map of the pebbly/lateritic sand

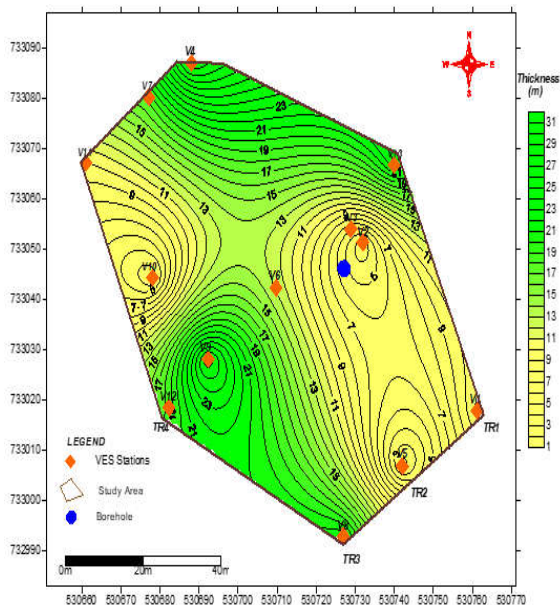


Fig. 14: Isopach Map of the pebbly/lateritic sand

The second order geoelectric parameter - longitudinal conductance (which is a Dar Zarrouk parameter) was evaluated from the first order parameters (thickness and resistivity) of the geoelectric layers which were used in the classification of the APC of the area. Highly impervious materials such as clay and shale usually have high longitudinal conductance values (resulting from their low resistivity values) while pervious materials such as sand and gravels have low longitudinal conductance values (resulting from their high resistivity values). While high longitudinal conductance value corresponds to excellent and good APC, low longitudinal conductance values are associated with poor and weak APC (Tables 2 and 3).

Table 2: Longitudinal Conductance/Protective Capacity Rating (Henriet, 1976).

Total Longitudinal Unit Conductance (MHOS)	Overburden Protective Capacity Classification
<0.10	Poor
0.1 - 0.19	Weak
0.2 - 0.69	Moderate
0.7 - 1.0	Good

Table 3: Modified Longitudinal Conductance/Protective Capacity Rating (Oladapo *et al.*, 2004)

Total Longitudinal Unit Conductance (MHOS)	Soil Protective Capacity Classification
>10	Excellent
5 - 10	Very Good
0.7 - 4.9	Good
0.2 - 0.69	Moderate
0.1 - 0.19	Weak
< 0.1	Poor

Table 4 presents the summary of the computation of total longitudinal conductance S and overburden protective capacity rating at all the thirteen VES stations in the study area. From the analysis (Table 4), the value of the total longitudinal unit conductance varies from 0.0164 - 0.1168 mhos in the study area and this signifies an overburden whose protective capacity is from poor to weak (Tables 2 and 3). This confirms the porous and permeable nature of the geologic materials (topsoil/pebbly sand/lateritic sand/clayey sand/silty sand) overlying the aquifer. Fig. 15 is the aquifer protective capacity map of the study area showing the spatial distribution of the longitudinal unit conductance across the study area. The north-eastern and western parts of the study area, accounting for 15% of the study area show areas with weak protective capacity ratings while other areas which represent 85% of the entire study area are characterized with poor protective capacity rating (Fig. 15). The weak and poor zones coincide with zones of shallow or thin overburden and relatively high electrical resistivity. These areas are vulnerable to easy and quick migration of near-surface/surface contamination sources. This result is in agreement with the interpreted or the inferred lithology across the study area for the overburden. From the interpreted geoelectric parameters, the inferred lithology for the layer directly overlying the aquifer is clayey sand/pebbly sand for the most parts of the study area. This lithologic unit is weak and porous in terms of its protective capacity and could offer little or no protection to the underlying aquifer as contaminating fluids can migrate relatively easy through this lithologic unit to pollute the aquifer.

Table 4: Total Longitudinal Unit Conductance (S) and Overburden Protective Capacity Rating

VES	Thickness of Layers (m)						Resistivity of Layers (Ωm)						Total Longitudinal Unit Conductance, $S = \sum_{i=1}^n \frac{h_i}{\rho_i}$ (mhos)	Overburden Protective Capacity Rating (after Henriet, 1976; Oladapo, et al., 2004)
	h_1	h_2	h_3	h_4	h_5	h_6	ρ_1	ρ_2	ρ_3	ρ_4	ρ_5	ρ_6		
1.	0.8	2.7	8.5	-	-	-	104	295	494	-	-	-	0.0341	Poor
2.	1.1	0.9	2.4	-	-	-	25	2526	498	-	-	-	0.0492	Poor
3.	1.0	2.2	3.9	28.2	-	-	36.0	346	1172	175	-	-	0.0204	Poor
4.	0.7	6.6	23.4	-	-	-	135	284	657	-	-	-	0.0640	Poor
5.	1.8	1.5	27.4	-	-	-	171	601	374	-	-	-	0.0268	Poor
6.	0.8	0.6	12.2	-	-	-	242	966	573	-	-	-	0.0252	Poor
7.	1.5	5.0	13.3	-	-	-	131	285	639	-	-	-	0.0498	Poor
8.	1.5	5.0	16.6	-	-	-	297	314	1185	-	-	-	0.0350	Poor
9.	1.0	4.6	22.2	-	-	-	140	569	638	-	-	-	0.0500	Poor
10.	1.7	3.0	38.9	-	-	-	156	610	391	-	-	-	0.1153	Weak
11.	0.7	0.6	6.4	2.9	-	-	132	539	361	968	-	-	0.0271	Poor
12.	0.9	1.0	7.5	9.8	20.3	-	250	902	270	724	265	-	0.0164	Poor
13.	0.6	5.9	17.0	-	-	-	15	176	393	-	-	-	0.1168	Weak

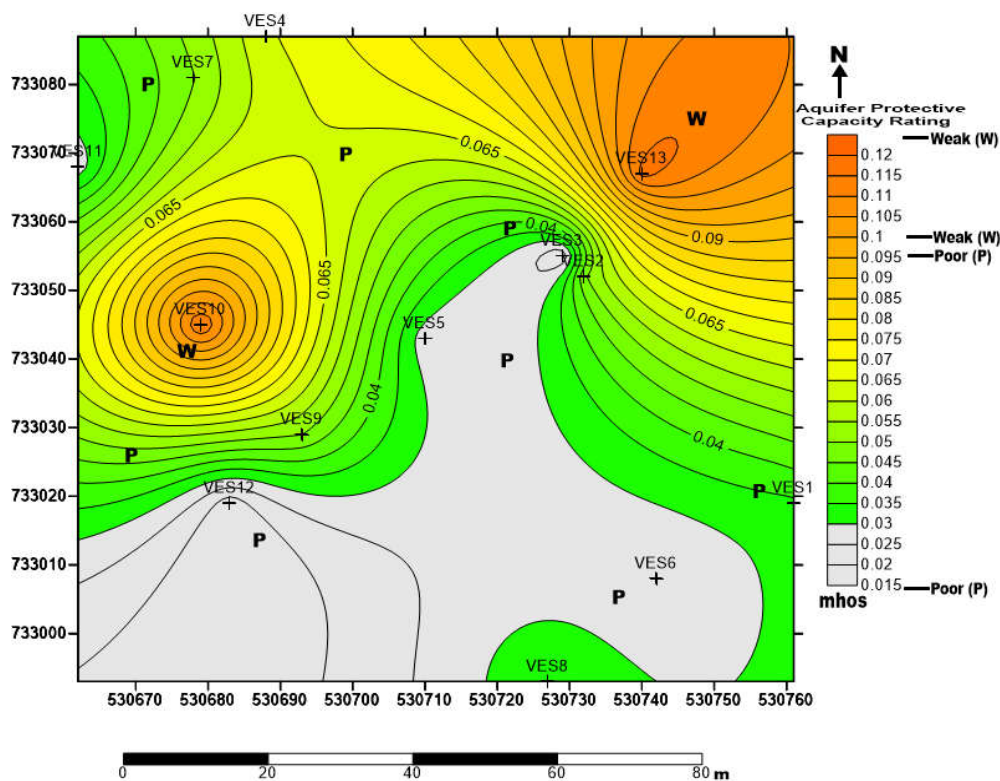


Fig. 15: Aquifer Protective Capacity Map of the Study Area

Conclusion: Due to expansion and self-sustainability, automobile mechanic settlement, abattoir and a meat processing factory have been proposed to be established at the Aboru Estate to serve as service facilities for the use of the increasing community. The operations of these service facilities such as the discharge of engine oil, blood and other fluids and solid materials are expected to impact the subsurface on the long-run with the high possibility of contamination and thereafter polluting the regional aquifer. As such, this necessitated a geophysical assessment (using Longitudinal Unit Conductance, S -

a Dar-Zarrouk parameter) of the vulnerability of the subsurface aquifers in the study area against the expected long-term anthropogenic impacts of these facilities on the groundwater system. The aquifer protective capacity map reveals that the north-eastern and Western parts of the study area show areas with weak protective capacity ratings while other areas in study are characterized with poor protective capacity rating. This indicates that the aquifers are poorly protected and thus the earth materials overlying the aquifers have a poor protective capacity rating. The establishment of the proposed service facilities such as

an automobile mechanic settlement, abattoir and a meat processing factory in the study area is strongly discouraged. The nature of the operations of these facilities has a high potential to contaminate and eventually pollute the sub-surface aquifers on the long-run. If however the inevitability of their establishment cannot be set-aside, secondary measures must be taken to forestall a direct impact of their operations on the subsurface.

Acknowledgement: The contributions of Mr. Akin-Ojo Tunji have been of immense help in improving the quality of this work.

REFERENCES

- AKO, BD; AJAYI, TR; ARUBAYI, JB; ENU, EI (2005). The Groundwater and its Occurrence in the Coastal Plains Sands and Alluvial Deposits of Parts of Lagos State. *Nigeria Water Res.*, 16: 7–17
- AKO, BD; OSONDU, VC (1986) Electrical Resistivity of the Kerri-Kerri Formation, Darazo, Nigeria. *J. Afri. Earth Sci.* 5(5): 527–534
- ABDULAZIZ, MA (2005). Resistivity Methods for Groundwater Exploration in the Cretaceous-Tertiary Sedimentary Sequence, East of Jeddah, Saudi Arabia. *J. Environ. Hydrology*, 13(19): 1–11
- ABIOLA, O; ENIKANSELU, PA; OLADAPO, MI (2009). Groundwater Potential and Aquifer Protective Capacity of Overburden Units in Ado-Ekiti, Southwestern Nigeria. *Intl. J. of Physical Sci.*, 4(3): 120–132
- ATAKPO, EA; AYOLABI, EA (2009). Evaluation of Aquifer Vulnerability and the Protective Capacity in Some Oil Producing Communities of Western Niger Delta. *Environmentalist*, 29: 310–317
- AYOLABI, EA (2005). Geoelectric Evaluation of Olushosun Landfill Site Southwest Nigeria and its Implication on Groundwater. *J. of Geol. Soc. of India*, 66: 318–322
- OMATSOLA, ME; ADEGOKE, OS (1981). Tectonic Evolution and Cretaceous Stratigraphy of the Dahomey Basin. *J. Mining Geology*. 18(1): 130–137
- BALOGUN, OY (2000). Senior Secondary Atlas. Longman, Nigeria Plc
- HASSANEIN, H; EL-KALIOUBY, H; AL-GARNI, MA (2007). The Use of DC Resistivity to Outline the Subsurface Hydrogeological and Structural Setting beneath a Proposed Site for Subsurface DAM Building, Makkah Al-Mukarramah, Saudi Arabia. *J. of King Abdul Aziz Univ. Earth Sci.*, 18(1): 117–138
- HENRIET, JP (1976). Direct Application of Dar-Zarrouk Parameters in Ground Water Surveys. *Geo. Pros.*, 24: 344–353
- KOGBE, CA (1976). The Upper Cretaceous Abeokuta Formation of Southwestern Nigeria, *Nigerian Field.* 4(47): 48–52
- LASHKARIPOUR, GR; SADEGHI, H; QUSHAEEI, M (2005). Vertical Electrical Soundings for Groundwater Assessment in Southeastern Iran: A Case Study. *J. of Appl. Geophys.*, 5(1): 973–977
- MAILLET, R (1947). The Fundamental Equation of Electrical Prospecting. *Geophy.* 12: 529–556
- OLADAPO, MI; MOHAMMED, MZ; ADEOYE, OO; ADETOLA, BA (2004). Geoelectrical Investigation of the Ondo State Housing Corporation Estate, Ijapo Akure, Southwestern Nigeria. *J. of Min. and Geol.*, 40(1): 41–48
- OLORUNFEMI, MO; FASUYI, SA (1993). Aquifer types, Geoelectric and Hydrogeologic Characteristics of Part of the Central Basement Terrain of Niger State Nigeria. *J. of Afri Earth Sci.*, 16(1): 309–317
- OLORUNFEMI, MO; OJO, JS; OLADAPO, MI (1998). Geological Hydrogeological and Geophysical Investigations of Exposed 20" Escravos Lagos Pipeline Technical Report
- SØRENSEN, KI; AUKEN, E; CHRISTENSEN, NB; PELLERIN, L (2005). An Integrated Approach for Hydrogeophysical Investigations: New Technologies and A Case History. In: Butler DK (ed) Near-Surface Geophysics Vol 2, Society of Exploration Geophysics, 585–603
- TELFORD, WM; GELDART, LP; SHERIFF, RE (1990). Applied Geophysics. Cambridge University Press, Cambridge.